Van der Waals Complexes of Jet-Cooled Aromatic Thiones with Noble Gases: The Phosphorescence Excitation Spectrum of 4*H*-Pyran-4-thione

A. A. Ruth*

Max-Planck-Institut für Biophysikalische Chemie, Abteilung Spektroskopie und Photochemische Kinetik, Am Fassberg 11, D-37077 Göttingen, Federal Republic of Germany

F. J. O'Keeffe,† M. W. D. Mansfield,† and R. P. Brint‡

Departments of Physics and Chemistry, National University of Ireland, University College, Cork, Ireland

Received: March 31, 1997; In Final Form: July 17, 1997⊗

The solvent spectral shifts of the $S_0 \rightarrow T_1$ origin bands of jet-cooled 4*H*-pyran-4-thione (PT) and 4*H*-1-benzopyran-4-thione (BPT) were observed in phosphorescence excitation spectra. Van der Waals complexes (1:1) of seed molecules with the carrier gas were observed in several rare gases. In all cases, the combination of a dispersive red-shift and a dipole−induced dipole blue-shift produced a total red-shift, up to a maximum of $\delta\tilde{\nu} = -21$ cm^{-1} for PT−Xe and $\delta\tilde{\nu} = -30$ cm^{-1} for BPT−Xe. Complexes of 1:*n* ($n > 1$) were not observable owing to the weakness of the direct $S_0 \rightarrow T_1$ transition. The inductive contributions to the shifts were calculated using values of excited-state dipole moments estimated from solution Stokes shifts; the dipole moments of both molecules in T_1 were found to be close to zero, significantly smaller than their ground-state dipole moments. The phosphorescence excitation spectrum of isolated PT is discussed in some detail. The electronic origin of T_1 at 16 844 cm^{-1} is assigned to the transition $S_{0,0} \rightarrow T_{1z,0}$; the transitions $S_{0,0} \rightleftharpoons T_{1(xy),0}$ are too weak to be detected with this method. Vibronic transitions $S_{0,0} \rightarrow T_{1z,v}$ in PT were analyzed up to excess energies of $\sim hc1450$ cm^{-1}.

1. Introduction

Van der Waals (vdW) complexes of aromatic molecules with rare gas atoms have been reported by many authors in recent years.[1−10] For the most part, the solvent spectral shift (SSS) due to *microsolvation* has been detected in strongly allowed transitions, where weak sidebands next to the main excitation band of the (unsolvated) molecule are observable. The formation of vdW complexes in an adiabatic expansion is dependent only on the expansion conditions (i.e. the type and pressure of the carrier gas, the nozzle diameter, the distance of the excitation zone from the nozzle, etc.) and is independent of the subsequent excitation process; the same fraction of seed molecules will be microsolvated prior to a forbidden process, as for an allowed one. Since $S_0 \rightarrow T_1$ transitions are generally very weak, detection of an even weaker sideband (by a factor of $\sim 10^{-2}$ or even less) presents obvious experimental challenges. It is not evident a priori whether a *measurable* solvent spectral shift of the triplet absorption energy of a thione is produced by microsolvation with a rare gas atom; the SSS could lie within the rotational envelope of the unsolvated band. vdW complexes involving aromatic thiones have been reported for the SSS of the strongly allowed $S_0 \rightarrow S_2$ transition of xanthione and 4*H*-1-benzopyran-4-thione (BPT).[9−11] Microsolvation shifts of spin-forbidden transitions have never been reported for thione compounds. In this paper an investigation of solvent spectral shifts in the $T_1 \rightarrow S_0$ phosphorescence excitation spectra of jet-cooled BPT and 4*H*-pyran-4-thione (PT) are presented, using direct $S_0 \rightarrow T_1$ excitation.

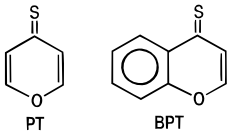

In the case of molecules with a permanent dipole moment, the total shift $\delta\tilde{\nu}$ consists of two components, a *dispersive* shift $\delta\tilde{\nu}_{\text{disp}}$ and a *dipole−induced dipole* shift $\delta\tilde{\nu}_{\text{ind}}$:

$$\delta\tilde{\nu} = \delta\tilde{\nu}_{\text{disp}} + \delta\tilde{\nu}_{\text{ind}} \tag{1}$$

The magnitudes of these two components are generally calculated using a perturbation model originally developed by Longuet-Higgins and Pople[12] to explain spectral shifts in liquid solvents but which has also been applied to vdW complexes:[3,9]

$$\delta\tilde{\nu}_{\text{disp}} = \frac{-\alpha'_{\text{A}} r^{-6}}{hc} \frac{\eta I_{\text{M}} I_{\text{A}}}{I_{\text{M}} + I_{\text{A}} - E_{\text{M}_i}} \left(\frac{3E_{\text{M}_i}\alpha'_{\text{M}}}{2(I_{\text{M}} + I_{\text{A}})} + \frac{|M_{0\rightarrow i}|^2}{4\pi\epsilon_0 (I_{\text{A}} - E_{\text{M}_i})} \right) \tag{2a}$$

$$\delta\tilde{\nu}_{\text{ind}} = -\frac{\alpha'_{\text{A}} r^{-6}}{2hc} \left(\frac{|\mu_i|^2 - |\mu_0|^2}{4\pi\epsilon_0} \right) \tag{2b}$$

Here, α' is the polarizability volume[13] (i.e. $\alpha' = \alpha/4\pi\epsilon_0$, where α is the polarizability). The indices M and A refer to the seed molecule and carrier gas atom, respectively. r is the equilibrium separation of the atom and molecule in the ground state. E_{M_i} is the energy of the relevant molecular transition. I_{A} and I_{M} are the ionization energies of the atom and molecule, and $M_{0\rightarrow i}$ is the dipole moment of the electronic transition. μ_0 and μ_i are the *permanent* dipole moments[14] of the molecule in its ground and excited state (i), respectively. η is an empirical factor, of

* Corresponding author. Present address: Department of Physics, National University of Ireland, University College, Cork, Ireland.
† Department of Physics.
‡ Department of Chemistry.
⊗ Abstract published in *Advance ACS Abstracts,* September 1, 1997.

S1089-5639(97)01120-1 CCC: $14.00

order unity, which is included to compensate for the inaccuracy involved in using I_M and I_A as average excitation energies in deriving eq 2a; this issue has been discussed at some length by Kettley et al.[3]

The dispersive shift $\delta\tilde{\nu}_{disp}$ is always negative (red-shift) and depends essentially on the transition moment, $M_{0\rightarrow i}$, of the excitation process. The sign of the dipole−induced dipole shift $\delta\tilde{\nu}_{ind}$ depends on the change in the permanent dipole moment on excitation. For an allowed transition, $\delta\tilde{\nu}_{disp}$ is usually considerably larger[4] than $\delta\tilde{\nu}_{ind}$, and the total shift $\delta\tilde{\nu}$ is therefore negative. For a forbidden singlet−triplet transition, however, with a much smaller transition moment, this is not necessarily true. In the $S_0 \rightarrow T_1(n,\pi^*)$ excitation of thiones one would expect a significant transfer of electron density from the S atom to the C═S bond and consequently a large reduction of the permanent dipole moment. Therefore the dipole−induced dipole shift is likely to make a significant contribution; the relative magnitudes of $\delta\tilde{\nu}_{disp}$ and $\delta\tilde{\nu}_{ind}$ determine the direction of the resulting SSS.

It is convenient to split expression 2a for the dispersive shift into two components, one dependent on the polarizability of the solute molecule, α'_M, the other on the transition dipole moment, $M_{0\rightarrow 1}$:

$$\delta\tilde{\nu}_{disp} = \delta\tilde{\nu}^{(1)}_{disp} + \delta\tilde{\nu}^{(2)}_{disp} \tag{3}$$

with

$$\delta\tilde{\nu}^{(1)}_{disp} = -\frac{\alpha'_A r^{-6}}{hc}\frac{\eta I_M I_A}{I_M + I_A - E_{M_i}}\frac{|M_{0\rightarrow i}|^2}{4\pi\epsilon_0(I_A - E_{M_i})} \tag{3a}$$

$$\delta\tilde{\nu}^{(2)}_{disp} = -\frac{\alpha'_A r^{-6}}{hc}\frac{\eta I_M I_A}{I_M + I_A - E_{M_i}}\frac{3E_{M_i}\alpha'_M}{2(I_M + I_A)} \tag{3b}$$

The relative magnitude, β, is given by

$$\beta \equiv \frac{\delta\tilde{\nu}^{(1)}_{disp}}{\delta\tilde{\nu}^{(2)}_{disp}} = \frac{|M_{0\rightarrow i}|^2}{6\pi\epsilon_0 E_{M_i}\alpha'_M}\frac{I_A + I_M}{I_A - E_{M_i}} \tag{4}$$

For an allowed transition, β is on the order of unity and both terms are significant.[15] In contrast, for singlet−triplet transition of aromatic thiones,[16] $\delta\tilde{\nu}^{(2)}_{disp}$ dominates and $\beta \approx 10^{-4}$. (Relevant atomic and molecular parameters in eqs 3 and 4 are listed in Table 4 for PT, BPT, and the rare gases.)

All of the solvation effects treated here are due to complexes of either PT or BPT with noble gas atoms. Complexes of 1:*n*, with *n* solvent atoms surrounding a solute molecule, are known for values of *n* up to 55,[17] with correspondingly (but not necessarily linearly) increased values of $\delta\tilde{\nu}$.[18] In this paper, however, only the $n = 1$ case will be discussed, as higher order complexes were not detected in the phosphorescence excitation spectra. The phosphorescence excitation spectrum of PT will be treated before the discussion of vdW complexes in section 3.

2. Experiment

The experimental setup for the LIP excitation measurements has been described in detail elsewhere (Figure 1 in ref 19). A circular stainless steel nozzle with a diameter of 0.8 mm was used to create the pulsed adiabatic expansion (General Valve Corporation, Iota One nozzle driver). Molecules in the jet were excited with an excimer-pumped pulsed dye laser (Lumonics EX-700, XeCl; Lumonics HD-300; rhodamine B, rhodamine 6G, coumarine 153). The phosphorescence was collected with two lenses at right angles relative to the jet and to the excitation laser beam. The emission was detected with a gated photomultiplier (Philips XP2254/B) in the photon-counting mode. The home-built gate of the PMT has a rise time of $\gtrsim 3$ μs and a width of 300 μs. The pulses from the photomultiplier were accumulated in a time window between 3 and 30 μs by a digital photon-counter (SRS-400), which was interfaced to a computer for the final data acquisition. Typical sampling rates were 100−200 shots per data point.

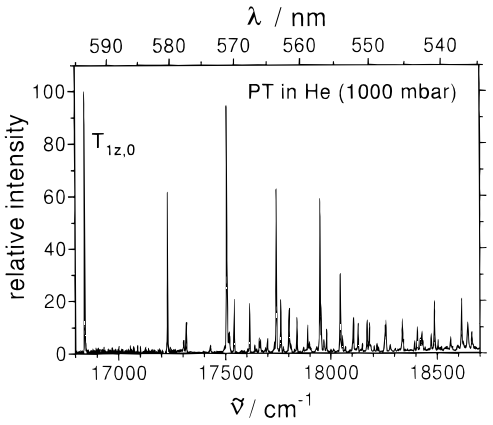

Figure 1. Normalized phosphorescence excitation spectrum of jet-cooled PT in the region of the $S_0 \rightarrow T_1$ absorption. The carrier gas is helium at a stagnation pressure of 1000 mbar. Wavelengths and wavenumbers are vacuum-corrected; relative intensities are not corrected with respect to the excitation fluence.

The synthesis and purification of the zone-refined PT and BPT are described in ref 20. For each of the two compounds different rare gases (He, Ne, Ar, Kr, and Xe) were used in turn as the carrier gas. The distance between the nozzle and the zone of excitation was varied between ∼10 and ∼30 mm so that the laser pulse would intercept the jet at different stages of the expansion. In this way the temperature and density of molecules were varied. The stagnation pressure of the carrier gases was in the range between 0 and 3 bar for He, Ne, and Ar and between 0 and 1 bar for Kr and Xe. The vapor pressure of the seed compounds was varied by adjusting the reservoir temperature between 20 and 35 °C for PT and between 70 and 90 °C for BPT, in order to change the relative proportions of seed molecules and carrier gas atoms in the jet.

No clear set of experimental conditions for 1:1 complex formation could be established. For each carrier gas, a different combination of backing pressure and position of the nozzle provided the best conditions for bringing the very weak complex peaks above the noise. Care was taken to distinguish solvation complex features from a difference hot band located 20 cm^{-1} below the $S_{0,0} \rightarrow T_{1z,0}$ transition in the BPT excitation spectrum (cf. section 3.2 in ref 19), particularly when the cooling conditions were not optimum (e.g. when He was used as the carrier gas at low pressures and the excitation zone was close to the nozzle). In most cases, due to the weakness of the solvation peaks, heavy saturation of the 0−0 peak (using maximum laser pulse energies) was necessary to make complex features detectable.

3. Results and Discussion

3.1. Phosphorescence Excitation Spectrum of Jet-Cooled 4*H*-Pyran-4-thione. The T_1 state of PT has been studied in solution and in rigid matrices by several groups in recent years.[21−25] However, the T_1 manifold of *isolated* PT has never been investigated. The phosphorescence excitation spectrum of jet-cooled PT is shown in Figure 1 in the region of the $S_0 \rightarrow T_1$ absorption (535−595 nm). The spectrum is expected to possess many properties similar to that of BPT, which was

TABLE 1: Comparison of the Fundamental Modes in T_1 (Column 3) with Modes and Symmetries from the S_0 Infrared Spectrum According to ref 29 (Column 2)[a]

label ref 29	$S_{0,v}$ (IR) [cm^{-1}] sym	$T_{1z,v}$ [cm^{-1}]	υ_{26} (b_2) [cm^{-1}]	υ_{25} (b_2) [cm^{-1}]	υ_9 (a_1) [cm^{-1}]	υ_8 (a_1) [cm^{-1}]	υ_7 (a_1) [cm^{-1}]
origin	ref 29	16 844	17 230	17 508	17 541	17 743	17 950
υ_{27}	94 b_2*						
υ_{22}	300 b_1^m						
υ_{13}	400 a_2^m	459.6 (w)	459.9 (w)	459.6 (w)	459.4 (w)	461.6 (w)	
υ_{26}	415 b_2*	385.7 (s)	384.8 (m)	382.8 (m)	386.8 (w)	385.3 (m)	386.7 (m)
υ_{10}	420 a_1^m	471.9 (m)	470.0 (w)	473.5 (m)	471.4 (w)	474.8 (w)	470.1 (w)
υ_{21}	648 b_1^m	673.0 (m)	673.1 (w)				672.1 (w)
υ_{25}	685 b_2^m	663.5 (s)	660.6 (m)	664.3 (m)	663.3 (w)	664.0 (m)	665.2 (m)
υ_9	722 a_1	697.3 (m)	698.4 (w)	697.1 (w)		698.9 (m)	695.7 (m)
υ_{12}	801 a_2*	793.8 (w)		794.7 (w)			
υ_{24}	814 b_2	815.0 (w)		815.8 (w)			
υ_8	918 a_1	899.0 (s)	898.6 (m)	899.5 (m)	900.6 (w)	899.4 (m)	
υ_{11}	953 a_2	958.4 (m)	956.8 (w)			960.0 (m)	
υ_{23}	963 b_2	995.2 (m)	995.4 (w)	996.5 (w)			
υ_7	1018 a_1	1105.4 (s)	1106.4 (m)	1107.1 (m)	1103.8 (m)		
υ_{20}	1021 b_1	1110.5 (m)	1111.1 (m)				
υ_6	1168 a_1	1202.2 (s)	1203.0 (w)	1204.6 (m)			
υ_5	1226 a_1	1212.0 (m)					
υ_{19}	1232 b_1	1263.3 (m)					
υ_{18}	1301 b_1	1337.7 (m)					
υ_{17}	1399 b_1	1412.1 (m)	1415.4 (m)				
υ_4	1426 a_1	1416.8 (m)					
υ_{16}	1548 b_1^m	1549.4 (m)					
υ_3	1646 a_1	(1719.1) (m)					

[a] * = calculated, m = melt. The most prominent progressions based on the vibronic origins υ_7, υ_8, υ_9, υ_{25}, and υ_{26} are given in columns 4−8. The difference between wavenumbers of fundamentals and combinations is $\lesssim 1$ cm^{-1}. Band intensities are classified as (s) = strong, (m) = medium, or (w) = weak.

communicated recently.[19,26] The electronic origin at 16 844 cm^{-1} is assigned to the transition $S_{0,0} \rightarrow T_{1z,0}$, since the transitions to the other electronic triplet substrates $S_{0,0} \rightleftharpoons T_{1(xy),0}$ are too weak to be detected with this method. The large zero-field splitting, which is known for PT in an *n*-pentane Shpolskii matrix ($|D^*| \gtrsim 24$ or 28 cm^{-1} depending on the trap site[21]) could not be investigated. Therefore the properties of the spectrum are entirely based on the triplet substrate T_{1z}. Szymanski et al.[27] estimated the energy origin of T_{1z} to be $E_{T_{1z}} \simeq$ hc17100 cm^{-1} in a perfluoro-1,3-dimethylcyclohexane (PFDMCH) solution, giving a hypsochromic shift of $\Delta\tilde{\nu}_{hyp}(PT) \approx 256$ cm^{-1}. In comparison, the triplet states of BPT in a PFDMCH solution[28] and in a supersonic jet expansion[19] are separated by $\Delta\tilde{\nu}_{hyp}(BPT) \approx 262$ cm^{-1}. This near-identical solvent blue-shift of the two compounds is probably coincidental.

The Observability of the $S_0 \rightarrow S_1$ Transition in Jet-Cooled PT. For BPT in a supersonic jet the energy gap between $S_{1,0}$ and $T_{1z,0}$ was found to be similar to the value measured in solution as determined by a multiphoton excitation spectrum ($\Delta\tilde{\nu}(S_1,T_1) \approx 690$ cm^{-1}).[26] In the single-photon excitation spectrum of BPT only an extremely weak feature was visible at the energy of $S_{1,0}$.[19] This observation was caused by the fact that no optical filtering was used in the experiment and a small fraction of blue $S_{2,v'} \rightarrow S_{0,v''}$ fluorescence was detected following a resonance-enhanced multiphoton excitation process $S_{0,0} \rightarrow S_{1,w'} \rightarrow S_{2,w'}$.[26] If the same behavior occurs in PT, one would expect the origin of S_1 to lie $\sim$600 cm^{-1} above $T_{1z,0}$ at $\sim$17 450 cm^{-1}, since no optical filtering was used in the phosphorescence detection of the excitation spectrum in Figure 1 either. In fact a very weak feature may be observed in Figure 1 at 17 429 cm^{-1}, which is 585 cm^{-1} above the T_1 origin. This line was not assigned as a T_1 mode because of its lack of intensity and because no combinations were found that could be based on it. However, assigning the line at 17 429 cm^{-1} as the S_1 origin is very tentative, and further measurements are required to clarify this point.

3.2. Vibrational Assignments of Jet-Cooled PT in T_1. The smaller size and the planar C_{2v} symmetry of PT indicate that its vibronic structure should be considerably simpler than that of BPT and other large aromatic thiones. An analysis of the structure can be attempted, particularly as there is a thorough analysis of the infrared spectrum and an assignment of all ground-state fundamentals.[29] The labeling of vibrational modes in the following is taken from this ground-state analysis. PT is expected to possess 27 fundamental modes: 19 in-plane (10 a_1 and 9 b_2) and 8 out-of-plane (3 a_2 and 5 b_1) modes. Four of the in-plane modes are C−H stretches with energies around $\sim hc3000$ cm^{-1} and are outside the range of the excitation spectrum. Transitions involving a_2 modes are symmetry-forbidden, although they could gain intensity through mixing with the nearby S_1 state of A_2 symmetry (despite the low density of $S_{1,v}$ states at low excess energies). Their first overtones are expected to be more intense than their fundamental modes. Noting these limitations the spectrum was analyzed for repeated patterns in the energy separations of bands in comparison with energies of the ground-state vibrations from ref 29. In total 20 fundamental modes are identified in the excitation spectrum. Several of these form vibronic origins of remarkably similar progressions, listed in Table 1.

We assume that there are no huge changes in vibrational energies between the S_0 and T_1 electronic states. PT is a reasonably large molecule and the nπ* electronic transition is most likely to effect vibrations localized in the C=S region, probably to an extent less than $\sim$15%. There is no evidence for T_1 modes corresponding to the two lowest energy S_0 modes at 94 and 300 cm^{-1}. Three S_0 and T_1 modes have energies between 380 and 460 cm^{-1}, well separated from others and therefore are assumed to correspond. One of the T_1 modes, at 459 cm^{-1}, is a weak transition in the spectrum with a strong overtone at 919 cm^{-1} and is therefore probably an a_2 mode. One of the corresponding S_0 modes at 400 cm^{-1} is of a_2 symmetry, which supports this assignment, even though the energy change is $\sim$15%; the S_0 value is purely calculational, which could account for this large change. The strong mode υ_{26} at 386 cm^{-1} probably corresponds to a ground-state vibration at 415 cm^{-1} of b_2 symmetry. Another argument for this

TABLE 2: Spectroscopic Data on the Vibronic Transitions $S_{0,0} \rightarrow T_{1z,v}$ of PT in an Expansion Using He as Carrier Gas[a]

no.	$\lambda(T_{1z,v})$ [nm]	$\tilde{\nu}(T_{1z,v})$ [cm^{-1}]	$\delta\tilde{\nu}(\upsilon_i - 0)$ [cm^{-1}]	$\lvert\Delta\tilde{\nu}\rvert$ [cm^{-1}]	relative intensity	T_1 assignments	
1	593.68	16 844.1	0.0		(s)	$T_{1z,0}$	
2	580.39	17 229.8	385.7		(s)	υ_{26}	b_2
3	577.91	17 303.7	459.6		(w)	υ_{13}	a_2
4	577.50	17 316.0	471.9		(m)	υ_{10}	a_1
5	571.18	17 507.6	663.5		(s)	υ_{25}	b_2 (b_1?)
6	570.87	17 517.1	673.0		(m)	υ_{21}	b_1 (b_2?)
7	570.08	17 541.4	697.3		(m)	υ_9	a_1
8	567.71	17 614.6	770.5	<1	(m)	$2\upsilon_{26}$	
9	566.96	17 637.9	793.8		(w)	υ_{12}	a_2
10	566.28	17 659.1	815.0		(w)	υ_{24}	b_2
11	565.30	17 689.7	845.6	<1	(w)	$\upsilon_{26} + \upsilon_{13}$	
12	564.98	17 699.7	855.7	1.9	(w)	$\upsilon_{26} + \upsilon_{10}$	
13	563.60	17 743.1	899.0		(s)	υ_8	a_1
14	562.95	17 763.6	919.5	<1	(m)	$2\upsilon_{13}$	
15	562.61	17 774.3	930.2	1.3	(w)	$\upsilon_{13} + \upsilon_{10}$	
16	561.72	17 802.5	958.4		(m)	υ_{11}	a_2 (?)
17	560.56	17 839.3	995.2		(m)	υ_{23}	b_2
18	558.96	17 890.4	1046.3	2.9	(m)	$\upsilon_{26} + \upsilon_{25}$	
19	558.57	17 902.9	1058.8	<1	(w)	$\upsilon_{26} + \upsilon_{21}$	
20	557.78	17 928.2	1084.1	1.1	(w)	$\upsilon_{26} + \upsilon_9$	
21	557.12	17 949.5	1105.4		(s)	υ_7	a_1
22	556.96	17 954.6	1110.5		(m)	υ_{20}	b_1
23	556.57	17 967.2	1123.1	<1	(w)	$\upsilon_{25} + \upsilon_{13}$	
24	556.14	17 981.1	1137.0	1.6	(m)	$\upsilon_{25} + \upsilon_{10}$	
25	555.53	18 000.8	1156.7	<1	(w)	$3\upsilon_{26}$	
25	555.53	18 000.8	1156.7	<1		$\upsilon_{13} + \upsilon_9$	
26	555.16	18 012.8	1168.7	<1	(w)	$\upsilon_{10} + \upsilon_9$	
27	554.13	18 046.3	1202.2		(s)	υ_6	a_1 (C═S)
28	553.83	18 056.1	1212.0		(m)	υ_5	a_1 (C═S)
29	553.42	18 069.2	1225.1	?	(w)	?	
30	552.26	18 107.4	1263.3		(m)	υ_{19}	b_1
31	551.62	18 128.4	1284.3	<1	(m)	$\upsilon_{26} + \upsilon_8$	
32	551.02	18 148.2	1304.1	1.1	(w)	$\upsilon_{26} + 2\upsilon_{13}$	
33	550.30	18 171.9	1327.8	<1	(m)	$2\upsilon_{25}$	
34	550.00	18 181.8	1337.7		(m)	υ_{18}	b_1
35	549.86	18 186.4	1342.4	1.7	(w)	$\upsilon_{26} + \upsilon_{11}$	
36	549.31	18 204.7	1360.6	2.0	(w)	$\upsilon_{13} + \upsilon_8$	
36	549.31	18 204.7	1360.6	<1	(w)	$\upsilon_{25} + \upsilon_9$	
37	548.91	18 217.9	1373.8	2.9	(w)	$\upsilon_{10} + \upsilon_8$	
38	548.68	18 225.6	1381.5	<1	(w)	$\upsilon_{26} + \upsilon_{23}$	
39	547.76	18 256.2	1412.1		(m)	υ_{17}	b_1 (a_1?)
40	547.62	18 260.8	1416.8		(m)	υ_4	a_1 (b_1?)

[a] $\lambda(T_{1z,v})$: center wavelength. $\tilde{\nu}(T_{1z,v})$: center wavenumber. $\delta\tilde{\nu}(\upsilon_i - 0) = \tilde{\nu}(T_{1z,v}) - \tilde{\nu}(T_{1z,0})$: energy of modes with respect to $T_{1z,0}$ in wavenumbers. $\lvert\Delta\tilde{\nu}\rvert$: difference between experimental values and combinations of fundamental modes assigned. Relative intensities of lines are classified as (s) = strong, (m) = medium, or (w) = weak. For lines at higher excess energies several assignments are conceivable within the error limit of ~2 cm^{-1}. Assignments of symmetries denoted with "?" are alternative possibilities. The labeling was taken from ref 29 (compare Table 1). Wavelengths and wavenumbers are vacuum-corrected.

assignment is the fact that the first strong progression listed in Table 1 is based on υ_{26}. The next eight S_0 modes (up to ~1000 cm^{-1}) are closely matched in energy by the proposed T_1 fundamentals. However, the T_1 mode at 664 cm^{-1}, though closer to υ_{21} (ground-state wavenumber 648 cm^{-1}), was assigned to a b_2 mode since it is stronger than its neighbor at 673 cm^{-1} and it is the vibronic origin of a strong progression. Therefore the T_1 fundamentals attributed to the lines υ_{25} and υ_{21} are interchanged with respect to their energies. The T_1 mode at 794 cm^{-1} is probably of a_2 symmetry, because it is weak and has a strong overtone at 1586 cm^{-1}; it matches the S_0 mode υ_{12} (a_2) at 801 cm^{-1}. The average change in energies between T_1 and S_0 for those matched modes is ~16 cm^{-1} with a range of 1−25 cm^{-1}, typically a 2% difference.

The next four S_0 modes between 1100 and ~1250 cm^{-1} are less well matched by the T_1 modes, average differences of ~56 cm^{-1} with a range of 14−89 cm^{-1}, typically a 5% difference, and the simple direct correspondence is less certain. However, support for our assignments is provided by the intensities of the bands in Figure 1. Given that the electronic transition is localized on the C═S group, then transitions exciting vibrations involving this group can be expected to be reasonably intense. Only five bands in the spectrum, other than the origin, are classified as strong lines. Of these the three lines υ_6, υ_{25}, and υ_{26} have been assigned by the above criterion to fundamental modes which in S_0 have significant C═S involvement. The three other S_0 modes localized on C═S, υ_5 and υ_9, correspond to medium-intensity vibronic lines in the phosphorescence excitation spectrum. There is no one S_0 mode that is purely C═S stretch and therefore almost certainly no one T_1 mode. The main C═S vibronic bands of the excitation spectrum are the strong υ_6 transition at 1202 cm^{-1} and the medium υ_5 transition at 1212 cm^{-1}. They are at a significantly lower energy than the corresponding feature in BPT at 1283.8 cm^{-1}.[30] The C═S stretch mode in PT carries a far smaller proportion of the oscillator strength of the $S_0 \rightarrow T_1$ transition than is the case for BPT. This suggests that PT undergoes a more significant distortion in the $S_0 \rightarrow T_1$ excitation process than BPT. Finally there is rather good correspondence between the energies of the last five modes (1263−1549 cm^{-1}), while the only match available for the S_0 mode ν_3 (a_1) at 1646 cm^{-1} is the T_1 energy at 1719 cm^{-1}, which we suspect is very uncertain. In Table 2 all significant lines in the measured excitation spectrum in Figure 1 up to an energy of ~1420 cm^{-1} above the origin are listed (40 features in total). Their assignments as either fundamental or combination of modes are also based on the comparison with

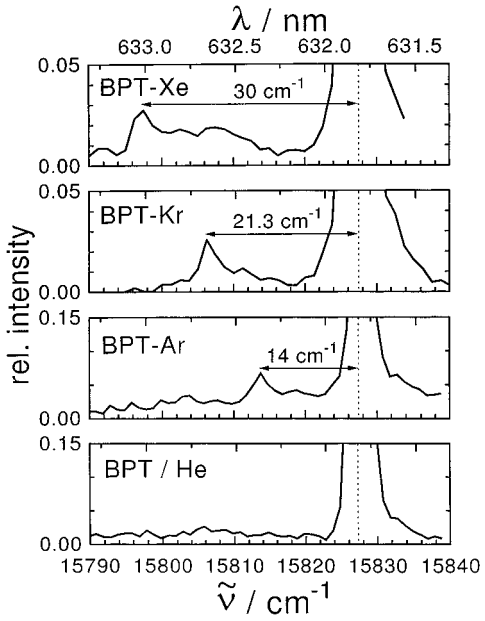

Figure 2. Solvent spectral shifts due to 1:1 complexes of BPT with Xe, Kr, and Ar. The trace on the bottom shows the unsolvated origin band in an expansion with He.

TABLE 3: Measured Solvent Spectral Shifts ($\delta\tilde{\nu}$) and Calculated Dispersive ($\delta\tilde{\nu}_{disp}$) and Dipole−Induced Dipole ($\delta\tilde{\nu}_{ind}$) Contributions for PT and BPT in Various Carrier Gases[a]

	spectral shifts					
complex	$\delta\tilde{\nu}$ [cm^{-1}]	$\delta\tilde{\nu}_{ind}$ [cm^{-1}]	$\delta\tilde{\nu}_{disp}$ [cm^{-1}]	$\Gamma_{A,M}$ [10^{26} m^{-3}]	$\lvert\delta\tilde{\nu}_{disp}/\Gamma_{A,M}\rvert$ [10^{-23} m^2]	η
BPT−Ar	−14	+35	−49	2.88	1.71	0.44
BPT−Kr	−21	+43	−64	3.67	1.74	0.45
BPT−Xe	−30	+50	−80	4.46	1.79	0.46
PT−Kr	−13	+45	−58	3.51	1.65	0.58
PT−Xe	−21	+54	−75	4.35	1.72	0.60

[a] $\Gamma_{A,M}$ was calculated using eq 6. η is the empirical factor used to derive $\delta\tilde{\nu}_{disp}$.

the ground-state vibrations using the respective labeling from Table 1. The only remaining line that could not be assigned is number 29 at 18 069 cm^{-1}.

3.3. Van der Waals Complexes of Thiones with Noble Gas Atoms. *4H-1-Benzopyran-4-thione.* The 0−0 band of the $S_0 \rightarrow T_1$ transition of jet-cooled BPT, using four different monoatomic carrier gases, is shown in Figure 2. A weak feature displaced to the low-energy side of the (unsolvated) main 0−0 transition is attributed in each case to an SS due to the formation of a 1:1 complex with an atom of the relevant carrier gas. The observed red-shifts, $\delta\tilde{\nu}$, which are listed in Table 3, are significantly smaller than the dispersive shifts $\delta\tilde{\nu}_{disp}$ expected from eq 2a, due to a substantial permanent dipole−induced dipole blue-shift. In general, it was found that vdW complexes were formed more consistently and in higher proportions for the larger rare gas atoms, as one would expect from the larger binding energies, which make positive contributions from *both* the dispersive and dipole−induced dipole interactions. Solvent shifts due to complexes with Xe and Kr were reasonably pronounced; 1:1 complex peaks with Ar were much weaker and were quite sensitive to variations in the backing pressure of the supersonic jet. In the case of Ne, a very weak feature at $\delta\tilde{\nu} = -11$ cm^{-1} was observed only with large sample sizes (1000 shots per data point) and was even then partially swamped by a neighboring difference hot band at $\delta\tilde{\nu} = -20$ cm^{-1}. For this reason, the assignment of an SSS to a BPT−Ne complex is too tenuous to be included in Table 3. We were unable to observe 1:1 complex formation with He or 1:*n* complexes ($n > 1$) with any rare gas in the phosphorescence excitation spectrum.

The measured values of $\delta\tilde{\nu}$ in Table 3 may be used to estimate the empirical factor η of eq 2a, if the ground-state, $|\mu_0|$, and excited-state, $|\mu_i|$, permanent dipole moments are known. An estimate of the magnitude of the excited-state dipole moment[31] may be made from the Stokes shift in solution, $\Delta\tilde{\nu}_{sol}$, according to Richert and Wagener:[32]

$$|\mu_i|(|\mu_0| - |\mu_i|) = \frac{8\pi\epsilon_0 chR_0^3(2\epsilon_r + 1)}{4\epsilon_r - 1}\Delta\tilde{\nu}_{sol} \qquad (5)$$

where R_0 is the hard-sphere radius of the solute molecule, and ϵ_r is the relative dielectric constant of the solvent.

The $S_0 \rightarrow T_1$ transition of BPT exhibits a Stokes shift of $\Delta\tilde{\nu}_{sol} \simeq 50$ cm^{-1} in PFDMCH,[28] whose static relative dielectric constant is $\epsilon_r = 1.863$.[33] The hard-sphere radius of a similar sized molecule, quinoxaline, was estimated to be $R_0 \approx 1.95$ Å by Richert and Wagener.[32] $|\mu_0|$ of BPT has not been measured, but Sinha et al.[34] suggest that it is likely to be slightly larger than the ground-state dipole moment of xanthione (2.9 D). A value of $|\mu_0| = 3.4 \pm 0.5$ D would therefore seem reasonable for BPT, considering also the measured values of the ground-state dipole moment of PT (see next section). Hence, the permanent dipole moment of BPT in T_1 was calculated using eq 5 to be very close to zero, $|\mu_{T_1}| \approx 0.35 \pm 0.35$ D. As the measured Stokes shift is so small, this value is relatively insensitive to variations in the values of $|\mu_0|$, R_0, and $\Delta\tilde{\nu}_{sol}$. The error in $|\mu_{T_1}|$ derives from the liberal error limits of $|\mu_0|$ and also of $R_0 = 2 \pm 0.5$ Å and $\Delta\tilde{\nu}_{sol} = 25-100$ cm^{-1} in the calculation, and allowing for a possible factor of 0.2 in eq 5, accounting for a more accurate approach in ref 32.[35] Owing to the small value of $|\mu_{T_1}|$, the change in dipole moment on excitation is $\Delta|\mu| = 3.1 \pm 0.8$ D. In comparison, Ludwiczak et al.[9] found $\Delta|\mu| \simeq 2$ D for the $S_0 \rightarrow S_2(\pi,\pi^*)$ transition in xanthione and suggest that this difference is slightly less for the same transition in BPT. CNDO/2-CI calculations by Capitanio et al.[36] indicate that the change in the permanent dipole moment of xanthione is substantially larger for the $n \rightarrow \pi^*$ transitions than for the $\pi \rightarrow \pi^*$ transitions. The value of $\Delta|\mu| \simeq 3.1$ D would therefore seem reasonable, and the second solution of the quadratic eq 5, which yields a value of $\Delta|\mu| \simeq 0$, can safely be rejected.

Since for singlet−triplet transitions $\delta\tilde{\nu}^{(1)}_{disp} \ll \delta\tilde{\nu}^{(2)}_{disp}$ ($\beta \approx 10^{-4}$), the total dispersive shift $\delta\tilde{\nu}_{disp}$ in eq 2a should virtually be proportional to the quantity $\Gamma_{A,M}$, given by

$$\Gamma_{A,M} = \frac{I_M I_A \alpha'_A}{(I_M + I_A - E_{M_i})(I_M + I_A)r^6} \qquad (6)$$

Relevant atomic and molecular parameters[37] are given in Table 4. Figure 3 shows a plot of $\delta\tilde{\nu}_{disp}$ versus $\Gamma_{A,M}$. A good degree of linearity is evident, as is confirmed by the near-constant values of $\delta\tilde{\nu}_{disp}/\Gamma_{A,M}$ for the three BPT−(rare gas atom) complexes in Table 3. From the slope in Figure 3 ($=1.96 \times 10^{-23}$ m^2) η is calculated to be $\simeq 0.51$ (the average of η yielded a value of 0.45, compare eq 7). As the value of $|\mu_{T_1}|$ used in the calculation is so close to zero, this is in fact an upper limit on η. In comparison, Kettley et al.[3] calculated values of $\eta = 0.32$ and $\eta = 0.42$ for the $S_0 \rightarrow S_1$ transitions of perylene and tetracene, respectively. The small value of the intercept in Figure 3 confirms the validity of the approximations used to derive η.

4H-Pyran-4-thione. Complex formation was observed in the $S_0 \rightarrow T_1$ LIP excitation spectrum of PT only with the carrier gases Kr and Xe. Figure 4 shows the appearance of the spectra containing peaks due to 1:1 complexes with these two gases.

TABLE 4: Atomic and Molecular Parameters Required for the Calculation of Solvent Spectral Shifts of Thiones[f]

	I [eV]	α' [Å^3]	r(PT)[c] [Å]	r(BPT)[c] [Å]	E_{MT_1} [eV]	$\lvert M_{0\rightarrow T_1}\rvert$ [10^{-30} C m]	$\lvert\mu_0\rvert$ [10^{-30} C m]
He	24.59	0.205					
Ne	21.56	0.395	3.00	2.99			
Ar	15.76	1.64	3.36	3.34			
Kr	14.00	2.52	3.50	3.47			
Xe	12.13	4.04	3.68	3.66			
PT	≃8[a]	11.3[b]			2.088	0.285[e]	12.1
BPT	≃8[a]	16.2[b]			1.962[d]	0.270[e]	11.4

[a] Ionization potentials of PT and BPT are not known, but are not expected to differ greatly from that of xanthione, estimated at 8 eV;[9] $\delta\tilde{\nu}_{disp}$ in eq 2a is relatively insensitive to I_M. [b] Estimate, using bond polarizability method in ref 37. [c] From ref 10. [d] From Table 1 in ref 19. [e] Calculated from $|M_{0\rightarrow T_1}|^2 = 3\epsilon_0 h\lambda^3\phi_p/16\pi^3\tau_p$. [f] I: ionization potential. α': polarizability volume. r: equilibrium intermolecular distance between rare gas and thione. E_{MT_1}: triplet state energy. $|M_{0\rightarrow T_1}|$: $S_0 \rightarrow T_1$ absorption transition moment. $|\mu_0|$: ground-state dipole moment.

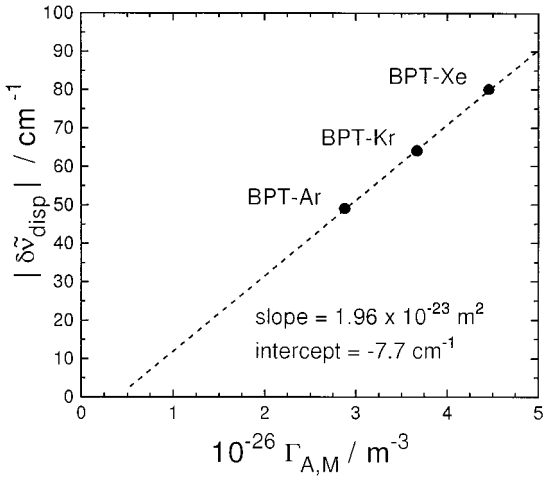

Figure 3. Plot of the dispersive shifts $|\delta\tilde{\nu}_{disp}|$ versus $\Gamma_{A,M}$ (cf. eq 6) for BPT.

As was the case with BPT, only 1:1 complexes were unambiguously observed. The measured spectral solvent shifts are shown in Table 3, together with calculated values of the dispersive and dipole−induced dipole contributions to each SSS. The lack of observable complex formation for He, Ne and Ar is probably due to a combination of two factors: (1) Microsolvation by the lighter rare gases is energetically less favorable, and therefore a smaller proportion of PT molecules form complexes. (2) The rotational envelopes of the $S_{0,0} \rightarrow T_{1z,0}$ transitions of PT and BPT are both reasonably wide, particularly under the heavily saturated excitation conditions required to enhance weak spectral features (depending on the expansion conditions, envelopes of up to 8−12 cm^{-1} were observed in some measurements). As the SSS of both compounds increases with the size of the carrier gas atom (cf. Table 3), and is smaller, for a given carrier gas, in the case of PT than for BPT, it is likely that the complex peaks of Ne and possibly Ar are contained within the line width of the unsolvated 0−0 band in the PT spectrum. The He complex peaks are almost certainly contained in the origin band in both the PT and BPT spectra.

Unlike BPT, two values for the ground-state dipole moment $|\mu_0|$ of PT have been measured: 3.95 ± 0.05 D[38] and 3.3 ± 0.3 D.[34] Accounting for both values, we used an average value with large enough error limits: $|\mu_0| \approx 3.6 \pm 0.5$ D. The triplet-state dipole moment, $|\mu_{T_1}|$, was then calculated from the Stokes shift in solution; Szymanski et al.[27] measured absorption and emission spectra of PT in 3-methylpentane (3MP), from which a Stokes shift of $\Delta\tilde{\nu}_{sol} \approx 130$ cm^{-1} can be estimated.[39] Taking a value of $R_0 = 1.5 \pm 0.5$ Å for the hard-sphere radius of PT

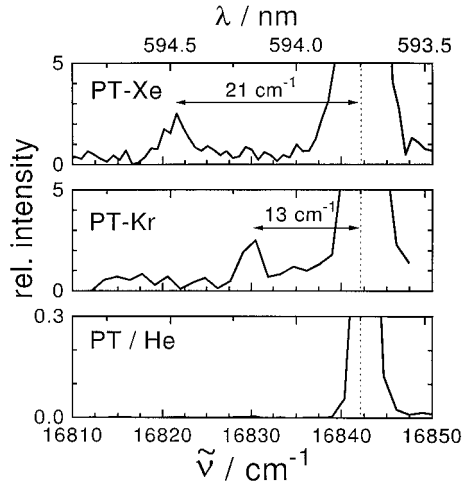

Figure 4. Solvent spectral shifts due to 1:1 complexes of PT with Xe and Kr. The trace on the bottom shows the unsolvated origin band in an expansion with He.

and a relative dielectric constant of $\epsilon_r(3MP) = 2.1$,[3] eq 5 gives $|\mu_{T_1}| \simeq 0.3 \pm 0.3$ D, similar to that of BPT (this value of the dipole moment, like the one for BPT, is the center value between the extremes of the error limits of the parameters used in the calculation). With this value of $|\mu_{T_1}|$ the shifts $\delta\tilde{\nu}_{ind}$ in Table 3 were calculated using eq 2b, and the values of $\delta\tilde{\nu}_{disp}$ required to produced the observed red-shifts were deduced. As only two closely spaced data points were available, no attempt was made to determine the slope of a linear fit to a plot of $\delta\tilde{\nu}_{disp}$ versus $\Gamma_{A,M}$ in order to estimate η. Instead, the average value of $\langle\delta\tilde{\nu}_{disp}/\Gamma_{A,M}\rangle_{ave} = 1.69 \times 10^{-23}$ m^2 (see Table 3) was used to calculate

$$\eta = \frac{2hc}{3E_{MT_1}\alpha'_M}\left\langle\frac{\delta\tilde{\nu}_{disp}}{\Gamma_{A,M}}\right\rangle_{ave} = 0.59 \qquad (7)$$

which is consistent with the value calculated for BPT (again, eq 7 is valid since $\beta \approx 0$ for $S_0 \rightarrow T_1$ transitions).

Comparison with $S_0 \rightarrow S_2$ LIF Microsolvation Shifts. The solvent spectral shifts of 1:1 complexes of the $S_0 \rightarrow T_1$ origins of PT and BPT are shown in Figure 5, together with the SSS of the $S_0 \rightarrow S_2$ origin of BPT, as measured by Sinha and Steer.[10] The data are plotted against α'_A/r^6, but one would not expect perfect linearity due to the I_A dependence of $\delta\tilde{\nu}_{disp}$ (eq 2a). As expected, the shifts of the S_2 origin are the greatest, due to the higher values of E_{MS_2} and $|M_{0\rightarrow S_2}|^2$, the latter making $\delta\tilde{\nu}^{(1)}_{disp}$ significant.

Assuming that the value of η is approximately the same for the $S_0 \rightarrow T_1$ and $S_0 \rightarrow S_2$ transitions in BPT, one would expect the dispersive shifts of the latter to be greater by a factor of approximately

$$\frac{\delta\tilde{\nu}_{disp}(S_0 \rightarrow S_2)}{\delta\tilde{\nu}_{disp}(S_0 \rightarrow T_1)} \approx [1 + \beta(S_2)]\frac{E_{MS_2}}{E_{MT_1}} \approx 2 \qquad (8)$$

while the dipole−induced dipole shift $\delta\tilde{\nu}_{ind}$ would be about the same ($\Delta|\mu|^2(S_0 \rightarrow T_1) \simeq 11$ D^2 and $\Delta|\mu|^2(S_0 \rightarrow S_2) \simeq 10$ D^2; for the latter value a dipole moment of $|\mu(S_2)| \approx 1.3$ D was assumed[34]). This would result in total red-shifts slightly larger than those observed by Sinha and Steer.[10] It is therefore likely that a smaller value of η is appropriate for the $S_0 \rightarrow S_2$ transition; a value of $\eta \simeq 0.36$ would be consistent with the data.

4. Conclusions

(i) The phosphorescence excitation spectrum of PT in a supersonic jet has been measured in the region of the $S_0 \rightarrow T_1$

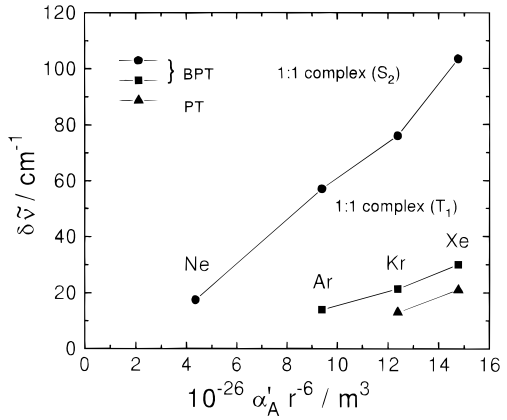

Figure 5. Comparison of solvent spectral shifts of the $S_{0,0} \rightarrow T_{1z,0}$ (■) and $S_{0,0} \rightarrow S_{2,0}$ (●) bands of BPT due to 1:1 complex formation with different noble gases. The solvent spectral shift of the $S_{0,0} \rightarrow T_{1z,0}$ band of 1:1 PT−(rare gas) complexes is shown on the bottom right (▼). All of the $S_0 \rightarrow S_2$ data are taken from ref 9.

absorption band. The electronic origin at 16 844 cm^{-1} is assigned to the transition $S_{0,0} \rightarrow T_{1z,0}$; the transitions $S_{0,0} \rightleftharpoons T_{1(xy),0}$ are too weak to be detected with the LIP excitation method.

(ii) In total 20 fundamental modes $T_{1z,v}$ were assigned for excess energies up to $\sim hc1450$ cm^{-1} above $T_{1z,0}$ (assignments above $\sim$1100 cm^{-1} are tentative).

(iii) The solvent spectral shifts of the $S_0 \rightarrow T_1$ origin bands of PT and BPT due to the formation of 1:1 thione−rare gas complexes were observed in several carrier gases. In all cases, the combination of a dispersive red-shift and a dipole−induced dipole blue-shift produced a total red-shift, up to a maximum of $\delta\tilde{\nu} = -21$ cm^{-1} for PT−Xe and $\delta\tilde{\nu} = -30$ cm^{-1} for BPT−Xe.

(iv) Complexes of 1:*n* ($n > 1$) were not observed owing to the weakness of the spin-forbidden direct $S_0 \rightarrow T_1$ excitation.

(v) The contributions to the shifts due to dipole−induced dipole interaction were calculated using values of excited-state dipole moments estimated from solution Stokes shifts; the dipole moments of both molecules in T_1 were found to be close to zero. The differences of the dipole moments between the ground and the triplet state were found to be $\Delta|\mu|(\mathrm{PT}) = 3.3 \pm 0.8$ D and $\Delta|\mu|(\mathrm{BPT}) = 3.1 \pm 0.8$ D.

(vi) An empirical factor, η, relating average excitation energies to the ionization energy of the molecules, was calculated to be 0.59 and 0.51 for the $S_0 \rightarrow T_1$ transitions of PT and BPT, respectively; for the $S_0 \rightarrow S_2$ transition of BPT, a value of $\eta \simeq 0.36$ was estimated.

Acknowledgment. We would like to thank Dr. B. Nickel (MPI für Biophysikalische Chemie, Göttingen, Germany) for providing various equipment, supplying pure PT and BPT, and for his encouraging interest in our work. This project was supported by the Irish organization for science and innovation FORBAIRT (contract SC/15/444), by the President's Research Fund of University College Cork, and through the Fonds der Chemischen Industrie im Verband der Chemischen Industrie Deutschland. A.A.R. gratefully acknowledges support by an EC fellowship (Human Capital and Mobility DG-XII, contract ER-BCHBGCT930368) and a Habilitationsstipendium provided by the Deutsche Forschungsgemeinschaft (contract RU672/1-1). We would like to thank one of the reviewers for bringing ref 29 to our attention.

References and Notes

(1) Leutwyler, S. *Chem. Phys. Lett.* **1984**, *107*, 284.
(2) Kettley, J. C.; Palmer, T. F.; Simons, J. P. *Chem. Phys. Lett.* **1985**, *115*, 40.
(3) Kettley, J. C.; Palmer, T. F.; Simons, J. P.; Amos, A. T. *Chem. Phys. Lett.* **1986**, *126*, 107.
(4) Bösiger, J.; Leutwyler, S. *Chem. Phys. Lett.* **1986**, *126*, 238.
(5) Kobayashi, T.; Honma, K.; Kajimoto, O.; Tsuchiya, S. *J. Chem. Phys.* **1987**, *86*, 1111.
(6) Troxler, T.; Knochenmuss, R.; Leutwyler, S. *Chem. Phys. Lett.* **1989**, *159*, 554.
(7) Leutwyler, S.; Bösiger, J. *Chem. Rev.* **1990**, *90*, 489.
(8) Shalev, E.; Ben-Horin, N.; Even, U.; Jortner, J. *J. Chem. Phys.* **1991**, *95*, 3147.
(9) Ludwiczak, M.; Sinha, H. K.; Steer, R. P. *Chem. Phys. Lett.* **1992**, *194*, 196.
(10) Sinha, H. K.; Steer, R. P. *J. Mol. Spectrosc.* **1997**, *181*, 194.
(11) Motyka, A. L.; Topp, M. R. *Chem. Phys.* **1988**, *121*, 405.
(12) Longuet-Higgins, H. C.; Pople, J. A. *J. Chem. Phys.* **1957**, *27*, 192.
(13) A factor of 3, implicit in the corresponding polarizabilities in ref 12, has been included explicitly in eqs 2a and 2b according to ref 3.
(14) All formulas in this paper are expressed in SI units; however, for convenience, dipole moments are also quoted in debyes (1 D = 3.36×10^{-30} C m).
(15) For example, for $S_0 \rightarrow S_2$ of BPT, with $|M_{0\rightarrow i}| = 15 \times 10^{-30}$ C m, $\alpha'_M = 16.2$ Å^3, $E_{MS_2} = 3.204$ eV, $I_M \approx 8$ eV, and I_A(argon) = 15.76 eV, the ratio is $\beta \approx 0.31$ (see Table 4).
(16) For most aromatics, β is several orders of magnitude smaller, in the absence of significant spin−orbit coupling.
(17) For 9,10-dichloroanthracene−$(Ar)_n$ complexes.
(18) Even, U.; Ben-Horin, N.; Jortner, J. *Chem. Phys. Lett.* **1989**, *156*, 138.
(19) Ruth, A. A.; O'Keeffe, F. J.; Brint, R. P.; Mansfield, M. W. D. *Chem. Phys.* **1997**, *217*, 83.
(20) Eisenberger, H. Dissertation, Göttingen, 1994.
(21) Taherian, M. R.; Maki, A. H. *Chem. Phys. Lett.* **1983**, *96*, 541.
(22) Maciejewski, A.; Safarzadeh-Amiri, A.; Verrrall, R. E.; Steer, R. P. *Chem. Phys.* **1984**, *87*, 295.
(23) Maciejewski, A.; Szymanski, M.; Steer, R. P. *J. Phys. Chem.* **1986**, *90*, 6314.
(24) Petrin, M. J.; Ghosh, S.; Maki, A. H. *Chem. Phys.* **1988**, *120*, 299.
(25) Szymanski, M.; Maciejewski, A.; Steer, R. P. *Chem. Phys.* **1988**, *124*, 143.
(26) Ruth, A. A.; O'Keeffe, F. J.; Mansfield, M. W. D.; Brint, R. P. *Chem. Phys. Lett.* **1997**, *264*, 605.
(27) Szymanski, M.; Steer, R. P.; Maciejewski, A. *Chem. Phys. Lett.* **1987**, *153*, 243.
(28) Eisenberger, H.; Nickel, B. *J. Chem. Soc., Faraday Trans.* **1996**, *92*, 733.
(29) Somogyi, Á.; Jalsovszky, G.; Fülöp, C.; Stark, J.; Boggs, J. E. *Spectrochim. Acta* **1989**, *45A*, 679.
(30) The C═S stretch for BPT in the ground state was found at 1250.0 cm^{-1} (IR),[10] for xanthione at 1240.7 cm^{-1} (Sinha, H. K.; Chantranupong, L.; Steer, R. P. *J. Mol. Spectrosc.* **1995**, *169*, 302).
(31) Here it is assumed that μ_0 and μ_i are parallel; in the case of PT, both moments lie along the C_2 axis. For BPT, this is not exactly true, but the calculated value of $|\mu_i|$ is so small that any error due to this assumption is insignificant.
(32) Richert, R.; Wagener, A. *J. Phys. Chem.* **1993**, *97*, 3146.
(33) Maciejewski, A. *J. Photochem. Photobiol. A* **1991**, *51*, 87.
(34) Sinha, H. K.; Abou-Zied, O. K.; Steer, R. P. *Chem. Phys. Lett.* **1993**, *201*, 433.
(35) Richert and Wagener[32] show that a mean spherical approximation (MSA) approach gives a more accurate estimate of the dielectric response than the Onsager continuum model (OCM), on which eq 5 is based. For given values of $|\mu_i|(|\mu_0| - |\mu_i|)$, the MSA method predicts Stokes shifts that are typically 3−5 times smaller than those predicted by the OCM theory. However, the MSA equations require an accurate value for the hard-sphere radius of the solvent molecule, which is not available for PFDMCH.
(36) Capitanio, D. A.; Pownall, H. J.; Huber, J. R. *J. Photochem.* **1974**, *3*, 225.
(37) Denbigh, K. G. *J. Chem. Soc., Faraday Trans.* **1940**, *36*, 936. Moelwyn-Hughes, E. A. *Physical Chemistry*; Pergamon: Oxford, 1961.
(38) Macdonald, J. N.; Mackay, S. A.; Tyler, J. K.; Cox, A. P.; Ewart, I. C. *J. Chem. Soc., Faraday Trans.* **1981**, *77*, 79.
(39) As with value was estimated from published graphs, it is only approximate; a large range of values (100−200 cm^{-1}) was allowed for in the calculation of $|\mu_{T_1}|$ to cater for this inaccuracy.